Solid State Communications, Vol. 55, No. 12, pp. 1075–1079, 1985.
Printed in Great Britain.

0038–1098/85 $3.00 + .00
Pergamon Press Ltd.

ANTI-STOKES RAMAN SCATTERING IN *TRANS* POLYACETYLENE

H. Eckhardt, S.W. Steinhauser and R.R. Chance

Corporate Research Center, Allied Corporation, Morristown, New Jersey 07960, USA

M. Schott

Groupe de Physique des Solides, Universite Paris VII, 75251 Paris, France

and

R. Silbey

Department of Chemistry and Center for Materials Science and Engineering, Massachusetts Institute of Technology, Cambridge, Massachusetts 02139, USA

(*Received* 28 *December*, 1984; *in revised form*, 17 *May*, 1985 *by E. Burstein*)

We report the first measurements of anti-Stokes Raman scattering in *trans* polyacetylene. The lineshapes are quite consistent with a disorder model in which the variation is attributed, for instance, to a disorder-induced distribution of conjugation lengths. The results suggest that the recently proposed hot luminescence model makes no significant contribution to the variation in the Raman lineshape with incident photon energy.

IT HAS BEEN KNOWN for some time that the Raman lineshape in *trans* polyacetylene varies dramatically with excitation wavelength [1–4]. This is especially true of the two vibrational modes at $\upsilon_1 = 1070\,\mathrm{cm}^{-1}$ and $\upsilon_2 = 1460\,\mathrm{cm}^{-1}$ which have mixed single and double bond character and both of which are strongly coupled to the main electronic excitation band. With excitation near the absorption edge ($\sim 12\,000\,\mathrm{cm}^{-1}$) a relatively narrow line is obtained for both these modes [5]. Excitation at higher energies, well into the absorption band, yields a sideband on the high frequency side of these Raman bands, which shifts to still higher frequencies as the excitation energy is increased. The initial explanation [2–4] put forward for this phenomenon, the disorder model, was that *trans* polyacetylene (PA) is composed of a distribution of conjugation lengths, i.e., the length over which conjugation is maintained without disruption by a chemical or structural defect. This explanation, which has important implications for all aspects of the electronic characterization of polyacetylene, has been questioned in recent work suggesting that hot luminescence in long chains is primarily responsible for this phenomenon [1].

In this paper we present for the first time results on anti-Stokes Raman scattering in *trans* PA. These data suggest that hot luminescence as described by Mele [1] makes no significant contribution to the Raman profiles. Our results are completely consistent with the disorder model and further emphasize the important role played by disorder in *trans* PA [6–8].

The electronic properties of *trans* PA, and other conjugated systems, extrapolate to those of the finite chain polymer with roughly a reciprocal chain length dependence, due to the increased delocalization of the π electron density with increasing chain length. The optical absorption frequency varies with conjugation length, n, approximately as [9–10]

$$\omega(n) = 12\,000 + 70\,000/n\,\mathrm{cm}^{-1}. \quad (1)$$

The Raman frequencies, designated υ_1 and υ_2 respectively, follow a similar empirical relationship. For example in the υ_2 case which has been most extensively studied, the variation is approximately [3]

$$\nu_2(n) = 1460 + 700/n\,\mathrm{cm}^{-1}. \quad (2)$$

In the disorder model, there is a distribution of conjugation lengths extending down to very small values of n. When the excitation frequency is near the absorption maximum for a segment of length n, the Raman profile will have an enhanced contribution from that segment due to the resonance Raman effect. In other words, that segment has been photoselected [9]. This basic model yields a fairly good (semi-quantitative) description of the Raman profiles and their variation with excitation frequency [2, 3]. To obtain a better fit to the experimental data other workers have used a $1/n^2$ dependence for long conjugation segments and a $1/n$ dependence for short segments [4]. A generalized version of the disorder model has been described by Vardeny *et al.* [11]. They show that a distribution in electron–phonon coupling

constants with normal Raman scattering processes (i.e., no hot luminescence) yields a reasonable fit to the Raman and infrared data, but do not discuss the physical origin of this distribution. We believe the physical origin of the disorder is most likely to be a distribution of conjugation lengths, this being most clearly the case with excitation below 600 nm [5]. In any case since the model of Vardeny *et al.* [11] deals with normal Raman processes, it is for our purposes indistinguishable from that based on a specific conjugation length distribution.

Mele [1] has suggested an alternative model to explain the Raman profiles which does not require disorder. *Trans* PA is assumed to consist only of very long conjugation length molecules; however the initially prepared wavepacket of the excited state is assumed to evolve prior to emission. This evolution results in an excitation energy dependent broadening of the lineshape. Thus the broadening is assigned to hot luminescence, not a Raman process. This model yields Raman profiles which agree qualitatively with experiment. Recently employing excitation profiles at various Raman frequencies, Lauchlan *et al.* [12] have lent their support to the hot luminescence (HL) model and have criticized the disorder model [13].

A qualitative illustration of the two competing models is shown in Fig. 1. For the disorder model, the process is just normal Raman scattering. Disorder produces a dispersion in the electronic and vibrational states, with photoselection via the resonance Raman effect enhancing the contribution on those states near the excitation frequency of the incident laser (ω_s). In the HL model for the Stokes case, two processes can be described which could yield scattered photons near (but removed from) the Raman line. If the energy relaxation involves excitation of low frequency lattice modes (v_L^*), we have case *a* in the figure. This process, discussed here by us but not considered by Mele, could yield the observed Stokes lineshape when ν_L^* is on the order of the observed Raman linewidth (about 100 cm^{-1}). In the second case, which has been treated in Mele's simulation [1] of the scattering process, the wavepacket evolution on the excited potential surface involves excitation of the vibrational mode v_1^*. Mele assumes that v_1^* has a similar dispersion to that calculated for the ground state v_1. In this case, emission is back to the ground state and the observed Raman lineshape is attributed to a combination of the normal Raman process with a sideband to lower energies determined by the $v_1^* - v_1$ difference.

Consider now the anti-Stokes Raman experiment. In the disorder model, the outgoing photon is $\omega_a' = \omega_a + v_1$, as illustrated in Fig. 1. Thus the anti-Stokes spectrum will be the mirror image of the Stokes spectrum. In the HL case, anti-Stokes scattering yields photons at $\omega_a' = \omega_a + v_1 - v_L^*$ in case *a* or $\omega_a' = \omega_a + v_1 - v_1^*$ in case *b*.

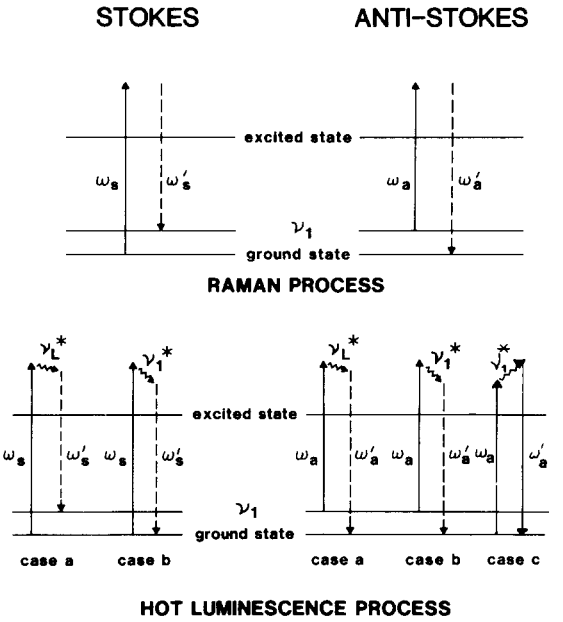

Fig. 1. Schematic diagram for Stokes and anti-Stokes scattering. At the top, the normal Raman processes are shown as they would be applied in the disorder model. For the hot luminescence process, case *a* represents energy relaxation via low frequency lattice modes so that $\omega_s' = \omega_s - v_L^*$ and $\omega_a' = \omega_a + v_1 - v_L^*$. In case *b*, the process considered explicitly by Mele [1], the energy relaxation is via excitation of v_1^* so that $\omega_s' = \omega_s - v_1^*$ and $\omega_a' = \omega_a + v_1 - v_1^*$. In case *c*, the anti-Stokes emission occurs after phonon absorption in the excited state so that $\omega_a' = \omega_a + v_1^*$.

The latter, considered in detail by Mele, will not yield any intensity near the anti-Stokes line. Case *a* in the HL model could yield appreciable intensity near the normal anti-Stokes line, but not with a mirror image relationship to the Stokes line.

There is an additional relaxation process which will yield anti-Stokes intensity, labeled *c* in the figure. Energetically this process is the opposite to that considered explicitly by Mele, in that a phonon is *absorbed* prior to emission, yielding an emitted photon at $\omega_a' = \omega_a + v_1^*$. The intensity of this emission will be proportional to the population of the state created when the phonon is absorbed while the intensity of the *Stokes* process (treated by Mele) will be proportional to the population of the state created when the phonon is emitted. The energy difference between these two states is $2hv_1^*$. At short times after excitation to the initial state, the populations will be determined solely by the dynamics of the molecule on the upper surface, so that the S/AS ratio would be the same as for the Raman process, i.e. $\exp(-hv_1^*/kT)$ or about 170 for the v_1 mode (1065 cm^{-1}). At long times after excitation, the populations will be determined by relaxation to

thermal equilibrium, so that the S/AS ratio would now be given by $\exp(-2h\nu_1^*/kT)$ since the emitting state for the Stokes process has energy $\omega_a - \nu_1^*$ while that for the anti-Stokes process is $\omega_a + \nu_1^*$. Thus the S/AS ratio for the case of a thermalized distribution in the HL model would be $\sim 3 \times 10^4$. The rate of vibrational relaxation which produces thermal equilibrium thus determines the S/AS ratio in the HL model. Vibrational relaxation processes are known to be fast (subpicosecond) in large organic molecules in condensed phases at the high temperatures of our experiments [15]. Moreover, the width of our lines imply that the experiment is sensitive to times on the picosecond scale. Thus the experiment should be in the intermediate time regime where the populations of the relevant states will be affected by relaxation processes; therefore, the S/AS ratio (in the HL model) is predicted to be intermediate between $\exp(-h\nu_1^*/kT)$ and $\exp(-2h\nu_1^*/kT)$.

Trans PA was obtained by dopant-induced isomerization of *cis*-rich PA films of approximately 100 μm thickness. This process has been shown to yield higher quality *trans* PA films than thermal isomerization [8]. Raman spectra were recorded in front surface scattering geometry with a Spectra Physics model 166 Argon ion laser and a Spex 1402 double monochromator. Since all experiments were carried out at room temperature, laser power was kept below 10 mW to avoid damage to the sample. A single scan was sufficient for a good signal-to-noise ratio in the Stokes mode; in the anti-Stokes mode typically 50 scans were averaged. We chose υ_1 for this investigation, since the intensity of the anti-Stokes emission is reduced by a Boltzmann factor, $\exp(-\nu/kT)$, compared to the Stokes emission. For υ_1, this translates to a factor of about 170 at 1065 cm^{-1}. (For υ_2, the factor would be about 1200.) We observe a Stokes/anti-Stokes ratio of about 200, as expected for normal Raman scattering and not nearly large enough for the relaxation-dominated HL model to be important.

Care must be taken in selecting the excitation frequency in the anti-Stokes experiment (ω_a) for comparison to the Raman lineshape obtained in a Stokes experiment at ω_s [16]. Within the disorder model we want to maintain at least approximately the same resonance conditions with the n distribution. Resonance effects will be important at both the excitation frequency and the scattered frequency, ω_s and $\omega_s - \upsilon_1$ for the Stokes experiment and ω_a and $\omega_a + \upsilon_1$ for the anti-Stokes experiment. Therefore, we expect resonance effects of the lineshapes to be roughly the same if we choose $\omega_s - \omega_a \sim \upsilon_1$. For cases *a* and *b* in the HL model, we want the state prepared by the excitation beam to be at the same energy in the Stokes and anti-Stokes experiments [1]; since excitation is from a vibrationally hot ground state (see Fig. 1), this is again best achieved with

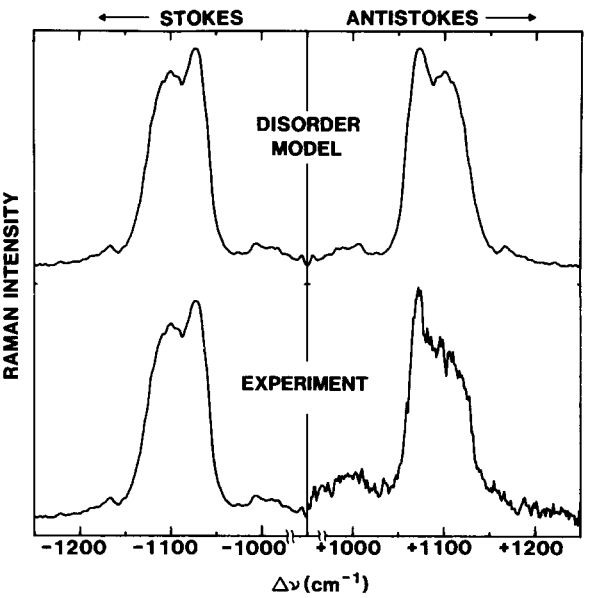

Fig. 2. Comparison of experiment and predictions of the disorder model for Stokes and anti-Stokes Raman scattering in *trans* polyacetylene. The Raman frequency, $\Delta\nu$, is defined as scattered light frequency minus the incident frequency. For the Stokes experiment the incident frequency is 20490 cm^{-1} (488.0 nm); for the anti-Stokes experiment the incident frequency is 19440 cm^{-1} (514.5 nm). On the Stokes side, the model curve is the same as the experimental; on the anti-Stokes side the model curve is generated as the mirror image from the experimental Stokes spectra, as described in the text. Note that the energy of the scattered light increases from left to right in this figure and in Fig. 2.

$\omega_s - \omega_a \sim \upsilon_1$. With the Argon laser lines available to us, this excitation condition is approximately met with ω_s at 488.0 nm and ω_a at 514.5 nm ($\omega_s - \omega_a = 1055$ cm^{-1}) and with ω_s at 447.9 nm and ω_a at 476.5 nm ($\omega_s - \omega_a = 852$ cm^{-1}). These excitation conditions are used in the experiments described here and provide a straightforward comparison of the models without the complications of absorption, reflection, and resonance corrections.

Results are shown in Figs. 2 and 3 along with the anti-Stokes spectra predicted with the disorder model. We have not generated the theoretical curves from first principles, but have instead generated the theoretical expectation for the anti-Stokes spectrum based on the lineshape of the experimentally observed Stokes spectrum. As pointed out above, the disorder model predicts that the anti-Stokes lineshape (due to the disorder-induced dispersion in υ_1 values) should be the mirror image of the Stokes lineshape, and the theoretical curves have been constructed accordingly for the figures.

A detailed calculation of the anti-Stokes spectrum in the HL model requires more than knowledge of the

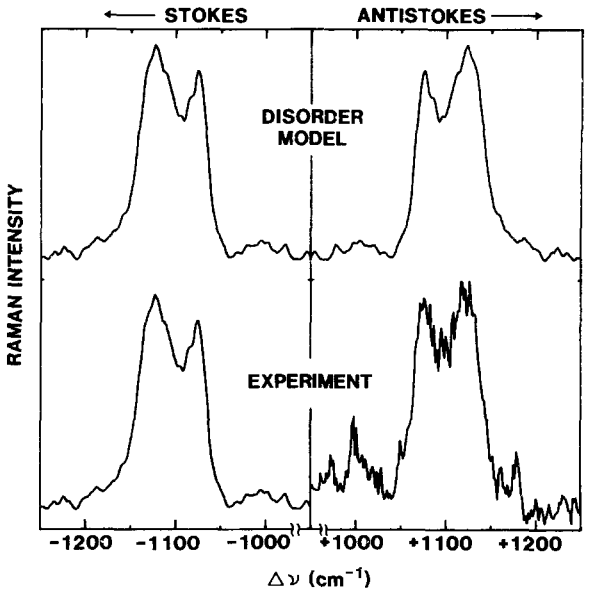

Fig. 3. Same as Fig. 2, except the Stokes incident frequency is 21 840 cm^{-1} (457.9 nm) and the anti-Stokes incident frequency is 20 990 cm^{-1} (476.5 nm).

Stokes spectrum. Nevertheless, a useful qualitative picture can be obtained. The HL model assumes that the initially absorbed photon excites the molecule electronically, but leaves the vibrational state unchanged. In case *a*, this vibrational state then relaxes and due to the electron–phonon coupling, scatters the electron from state to state while losing energy to the lattice. In case *b*, the state relaxes by emitting a v_1^* phonon and fluoresces to return to the ground state (Fig. 1). Clearly, the initially prepared vibrational state will differ in the anti-Stokes experiment from the Stokes experiment, since in the former case the initially prepared state has one quantum of ground state vibrational energy. In addition, there will be a distribution of vibrational states in the anti-Stokes experiment due to the large density-of-states of excited vibrational levels. All of these factors make the anti-Stokes spectrum difficult to calculate in the HL model. However, it is clear that independent of the initial state, cases *a* and *b* in the HL model predict relaxation of the population so that the outgoing photons will be largely of *lower energy* than those from the unrelaxed molecules. For case *a* in Fig. 1, the qualitative prediction in the HL model would be that the hot luminescence would appear as a sideband on the low energy side of the anti-Stokes line, whereas the experiment yields a sideband on the *high energy* side. For case *b* described by Mele [1], no sideband is expected, whereas the experiment yields a sideband very similar to that observed in the Stokes mode. As already noted in case *c*, the intensity is expected to be lower by a factor between 10^{-3} and 10^{-5} from the Stokes intensity, whereas our experiment yields about 10^{-2}. There is still one way the HL model could yield the observed ratio: if, for some unknown reason, vibrational relaxation in this sytem is extremely slow even at these temperatures. Although we cannot rule this out, we believe it to be unlikely.

The choice between the two models is clearly in favor of the disorder model. The experimental curves are in close agreement with the curves predicted with the disorder model, the agreement being well within that which could be expected with our approximation of identical resonance conditions for the Stokes and anti-Stokes experiments [17]. There is no evidence for hot luminescence on the rising edge of the anti-Stokes emission (low energy side). Therefore we conclude that the disorder model offers a good description of Raman scattering in *trans* PA and that hot luminescence makes no significant contribution to the Raman lineshapes.

We believe the evidence for substantial disorder in *trans* PA is now overwhelming. This has important consequences for the doping process particularly if the disorder is due to distribution of a conjugation lengths. The latter remains to be proven, but is the most appealing hypothesis at this stage. The doping process could be substantially affected if the shorter conjugated segments are not randomly distributed in the sample but for example are located preferentially on the surface of the fibers [18]. These shorter segments (on the surface or in the bulk) would not only interfere with intrachain carrier transport for obvious reasons, but also would be less easy to ionize than the longer chains [19]. If their concentration is as large as previous analyses of Raman experiments have suggested [2–4], substantial effects on the kinetics and energetics of the doping process can be expected.

Acknowledgements – We thank Ray Mariella, Jr. and E.J. Mele for helpful comments and suggestions. We also acknowledge the Regional Laser Laboratory at the University of Pennsylvania where the initial experiments were done.

REFERENCES

1. E.J. Mele, *Solid State Commun.* **44**, 827 (1982); *Phys. Rev.* **B26**, 6901 (1982); *J. Physique* **44**, 267 (1983).
2. L.S. Lichtmann, D.B. Fitchen & H. Temkin, *Synth. Met.* **1**, 139 (1979).
3. H. Kuzmany, *Phys. Status Solidi (b)* **97**, 521 (1980); F.B. Schuegerl & H. Kuzmany, *J. Chem. Phys.* **74**, 953 (1981); H. Kuzmany, E.A. Imhoff, D.B. Fitchen & A. Sarhangi, *Phys. Rev.* **B26**, 7109 (1982).
4. G.B. Brivio & E. Mulazzi, *Chem. Phys. Lett.* **95**, 555 (1983); E. Mulazzi & G.B. Brivio, *Molec. Cryst. Liq. Cryst.* **105**, 233 (1984).

5. J. Berrehar, J.L. Fave, C. Lapersonne-Meyer, M. Schott & H. Eckhardt, *Proceed. Int. Conf. Phys. and Chem. Synth. Met., Abano Terme, Italy 1984*; *Molec. Cryst. Liq. Cryst.* **117**, 393 (1985).
6. C.B. Duke, A. Paton & W. Salaneck, *Molec. Cryst. Liq. Cryst.* **83**, 177 (1982).
7. H. Eckhardt, *J. Chem. Phys.* **79**, 2085 (1983).
8. H. Eckhardt & S. Steinhauser, *Molec. Cryst. Liq. Cryst.* **105**, 219 (1984).
9. M.L. Shand, R.R. Chance, M. LePostollec & M. Schott, *Phys. Rev.* **B25**, 4431 (1982).
10. M.F. Granville, B.E. Kohler & J.B. Snow, *J. Chem. Phys.* **75**, 3765 (1981).
11. Z. Vardeny, E. Ehrenfreund, O. Brafman & B. Horowitz, *Phys. Rev. Lett.* **51**, 2326 (1983).
12. L. Lauchlan, S.P. Chen, S. Etemad, M. Kletter, A.J. Heeger & A.G. MacDiarmid, *Phys. Rev.* **B27**, 2301 (1983).
13. We do not accept the arguments of [12] for several reasons: (1) In his thesis Imhoff [14] has pointed out the problems associated with the correction of Raman spectra for the optical constants of $(CH)_x$. The main argument in [12], the flatness of the 1510 cm^{-1} excitation profile, appears to be an artifact of the adopted correction procedure. The complex morphology of the sample, the correct specular reflectance [7] and the presence of diffuse scattering [18] all have to be taken into account to arrive at reliable excitation profiles. (2) The failure to extend the measurements to high frequencies where short chains make their maximum contribution seriously compromises the conclusions of [12]. (3) The complications introduced into excitation profiles at different Raman frequencies ("sliced" profiles) by large intrinsic linewidths are neglected. These large linewidths lead to overlapping contributions at any given Raman frequency from various species (chain lengths) within the inhomogeneous distribution. For example, the Raman linewidth is about 25 cm^{-1} with red excitation (long chains only) and only about 70 cm^{-1} with blue excitation (see Figs. 2–3).
14. E.A. Imhoff, Ph.D. Thesis, Cornell University 1983.
15. W.H. Hesselink & D.A. Wiersma, *J. Chem. Phys.* **73**, 648 (1980); W.H. Hesselink & D.A. Wiersma, *Spectroscopy and Excitation Dynamics of Condensed Molecular Systems*, (Edited by V.M. Agranovich & A.M. Hochstrasser), p. 249, North Holland, (1983).
16. K.T. Schomacker, O. Bangcharoenpaurpong & P.M. Champion, *J. Chem. Phys.* **80**, 4701 (1984).
17. Note also that if we make a Boltzmann correction to the anti-Stokes spectra, the agreement with the disorder model is improved. For example, the intensity at 1110 cm^{-1} would be increased by about 25% with respect to that at 1065 cm^{-1} by this correction.
18. H. Eckhardt & R.R. Chance, *J. Chem. Phys.* **79**, 5698 (1983).
19. J.L. Brédas, R. Silbey, D.S. Boudreaux & R.R. Chance, *J. Am. Chem. Soc.* **105**, 6555 (1983).